Target Recognition of Apocalmodulin by Nitric Oxide Synthase I Peptides†

Petra Censarek,‡ Michael Beyermann,§ and Karl-Wilhelm Koch*,‡

Institut für Biologische Informationsverarbeitung 1, Forschungszentrum Jülich, D-52425 Jülich, Germany, and Foschungsinstitut für Molekulare Pharmakologie, Robert-Rössle-Strasse 10, D-13125 Berlin, Germany

Received February 14, 2002; Revised Manuscript Received May 17, 2002

ABSTRACT: An increasing number of proteins are found that are regulated by the Ca^{2+}-free state of calmodulin, apocalmodulin. Many of these targets harbor a so-called IQ motif within their primary sequence, but several target proteins of apocalmodulin lack this motif. We investigated whether the Ca^{2+}-dependent calmodulin-binding site of nitric oxide synthase I could be transformed into a target site of apocalmodulin. Synthetic peptides representing the wild-type amino acid sequence and several peptides carrying mutations were studied by isothermal titration calorimetry and fluorescence spectroscopy. A single amino acid substitution of a negative charge to a positive charge can convert a classical Ca^{2+}-dependent binding site of calmodulin into a target site for apocalmodulin. In addition, the introduction of hydrophobic amino acids increases the apparent binding affinity from the micromolar to the nanomolar range. Binding of wild-type and mutant peptides to Ca^{2+}-calmodulin was enthalpically driven, and binding to apocalmodulin was entropically driven. Our data indicate that only a few selected amino acid positions in a calmodulin-binding site determine its Ca^{2+} dependency.

Calmodulin (CaM)[1] is a ubiquitous modulator of enzymes and proteins. It belongs to the EF-hand superfamily of Ca^{2+}-binding proteins and regulates a variety of cellular processes. Most targets of CaM become activated when the intracellular Ca^{2+} concentration rises above the resting level of 0.1 μM. Ca^{2+}-bound CaM binds to a specific CaM-binding domain whereby it regulates the activity of the corresponding protein. In addition, there is an increasing number of proteins that are regulated by CaM in a Ca^{2+}-independent way (*1*, *2*). Therefore, targets of CaM can be classified according to whether they bind to the Ca^{2+}-bound state of CaM or to the Ca^{2+}-free state (ApoCaM). Different sequence motifs for a Ca^{2+}-dependent and a Ca^{2+}-independent interaction with CaM have been identified. The 1-8-14 and 1-5-10 motifs represent a Ca^{2+}-CaM-binding site, wherein the numbers indicate the position of hydrophobic residues. Most of these binding regions have a tendency to form a basic amphipathic α-helix consisting of approximately 20 amino acids (*3*, *4*). Ca^{2+}-independent binding of CaM to targets often occurs in proteins with an IQ motif, IQxxxRGxxxR (*1*, *2*).

Although most targets of CaM correspond to these three categories, several examples are known that do not match the above criteria. For example, the IQ motif in the insulin receptor substrate 1 shows a Ca^{2+}-regulated binding of CaM (*5*), or the inducible (macrophage) nitric oxide synthase type II (NOS-II) has a classical 1-8-14 motif but shows a Ca^{2+}-independent high-affinity binding to CaM (*6*). In contrast, the other nitric oxide synthase isoforms (NOS-I and NOS-III) are regulated by CaM in a reversible and Ca^{2+}-dependent manner (*7*).

Synthetic peptides corresponding to the CaM-binding site of NOS-I and NOS-III bound CaM reversibly with a similar affinity as the whole enzyme (*8*−*11*). Several investigators therefore concluded that the Ca^{2+}-dependent binding of CaM to NOS-I and NOS-III occurs within this region of 20−25 amino acids. Peptides derived from the putative CaM-binding domain of NOS-II showed CaM binding in the presence and absence of Ca^{2+} in several binding studies (*11*−*15*). However, another study reported no binding of CaM to the NOS-II peptide in the absence of Ca^{2+} (*16*).

The CaM-binding sites of NOS-I and NOS-II differ remarkably in a few amino acid positions. It is unclear how critical these positions are for the affinity and the Ca^{2+} dependency of binding to CaM. To resolve these questions we synthesized several peptides representing CaM-binding sites with point mutations at putative critical positions. We focused on amino acid substitutions that can change the amphipathic character of peptides. Interaction of CaM and ApoCaM with peptides was investigated by isothermal titration calorimetry and fluorescence spectroscopy. We here show that a single amino acid substitution from a negatively charged to a positively charged residue can create a binding site for ApoCaM.

EXPERIMENTAL PROCEDURES

Peptide Synthesis. Peptides were synthesized, purified, and characterized as described (*11*). Purity was ≥95% by HPLC analysis. The concentration of peptides was determined by measuring the absorption of the peptide bond at 205 nm using the formula $c(\text{mg/mL}) = A_{205} \times d/\epsilon$, where d is 1 cm and ϵ

† Supported by the Deutsche Forschungsgemeinschaft (Ko948/5-2; 5-3).

* Corresponding author. Tel: 49-2461-61-3255. Fax: 49-2461-614216. E-mail: k.w.koch@fz-juelich.de.

‡ Institut für Biologische Informationsverarbeitung 1, Forschungszentrum Jülich.

§ Foschungsinstitut für Molekulare Pharmakologie.

[1] Abbreviations: CaM, calmodulin; ApoCaM, Ca^{2+}-free calmodulin; NOS-I, nitric oxide synthase type I; ITC, isothermal titration calorimetry; dansyl, 5-(dimethylamino)naphthalene-1-sulfonyl.

10.1021/bi025681k CCC: $22.00
Published on Web 06/12/2002

is 31 (*17*). All peptides were also synthesized as a variant with an additional Cys at the NH_2 terminus. In this case the concentration of peptide stock solution was verified by determination of free sulfhydryl groups with DTNB [5,5′-dithiobis(2-nitrobenzoic acid)] (*18*). Peptide solution was diluted 10 times in 100 mM NaH_2PO_4/Na_2HPO_4 buffer, pH 8.0, and mixed with 2.5 mL of buffer and 50 μL of DTNB (4 mg/mL). After 15 min incubation at room temperature, the absorbance at 412 nm was measured. A standard curve was created with L-cysteine.

Isothermal Titration Calorimetry (ITC). Principles of experimental design and theory of data analysis of ITC have been described (*19*−*22*). We used a VP-ITC MicroCalorimeter from MicroCal Inc. (kindly provided by Prof. M. Bott, IBT, Forschungszentrum Jülich). The instrument consists of a sample cell, a reference cell, and a spinning syringe. One binding partner is in the sample cell and the other (reactant) in the spinning syringe. The calorimeter determines the temperature difference between the sample cell and the reference cell. The reactant is injected into the sample cell which leads to evolution or absorption of heat pulses in cases where a binding reaction occurs. The binding enthalpy and the equilibrium constant can be derived from a titration experiment, where the concentration of one binding partner is kept constant in the sample cell and the concentration of the reactant is increased by repetitive injections. Peptides and CaM were dissolved in water and diluted in buffer to a final concentration of 200 and 8 μM, respectively. Titration steps were 0.5 or 1 nmol per injection. The buffers contained 10 mM Hepes, pH 7.4, 150 mM NaCl, 10 mM $MgCl_2$, 3 mM $CaCl_2$, 2 mM EGTA, and 0.005% (v/v) Tween 20 (Ca^{2+} buffer) or 10 mM Hepes pH 7.4, 150 mM NaCl, 2 mM $MgCl_2$, 10 mM EGTA, and 0.005% (v/v) Tween 20 (EGTA buffer). All measurements were done at 25 °C. Data analysis was done with Microcal Origin Version 5.0.

Protein Determination. CaM stock solutions were prepared from a lyophilized powder purchased from Sigma. The protein concentration was determined by a Coomassie Blue dye binding assay (*23*) using a CaM standard curve. The concentration of CaM standards was adjusted by using the molar extinction coefficient of CaM at 277 nm of $\epsilon = 3006$ M^{-1} cm^{-1}. Alternatively, the BCA protein assay reagent kit from Pierce was used. Bicinchoninic acid and $CuSO_4$ were mixed at a ratio of 50:1. Samples were adjusted to a concentration of 20−40 μM, and 50 μL was mixed with 1 mL of the Cu^{+}−bicinchoninic acid complex. The mixture was incubated at 60 °C for 30 min and then measured at 562 nm at room temperature (*24*). A standard curve was created with bovine serum albumin.

Dansylation of Calmodulin. CaM was derivatized with dansyl chloride according to a published procedure (*25*) with some modifications. CaM (50000 units) was dissolved in dansylation buffer (20 mM Na_2CO_3, pH 10, 100 mM NaCl, 250 μM $CaCl_2$). Dansyl chloride was dissolved in water-free acetone (1 mg/mL). The CaM solution was slowly mixed with 25 μL of dansyl chloride and incubated in the dark for 1.5 h. Afterward, the buffer was changed to a Hepes/NaCl buffer (10 mM Hepes, pH 7.4, 150 mM NaCl) using a NAP-5 column. The grade of dansylation was determined as described (*25*). Two charges of dansylated CaM were used (0.59 mol of dansyl chloride/mol of CaM and 0.87 mol of dansyl chloride/mol of CaM).

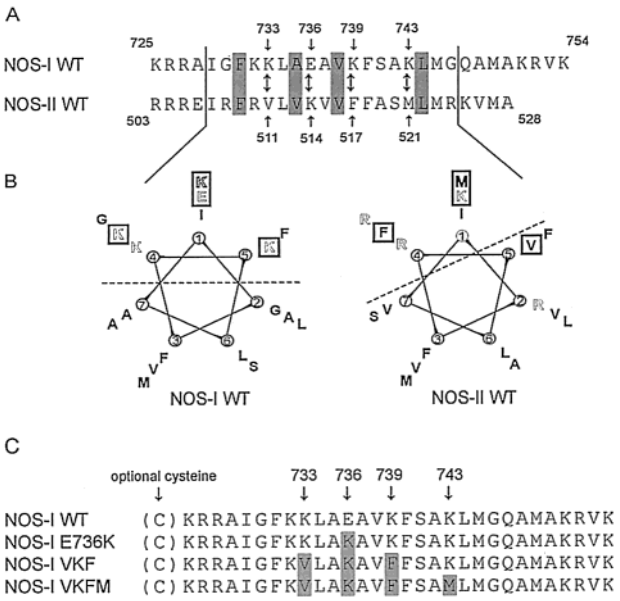

FIGURE 1: (A) Wild-type (WT) amino acid (aa) sequence of NOS-I (human or rat) and -II (mouse macrophage) CaM-binding sites. The conserved hydrophobic aa are highlighted in gray. The nonconservative aa exchanges are marked by arrows. (B) Schiffer−Edmundsen diagram of the CaM-binding sequences. Charged aa are shown as open letters; the four critical residues are shown in boxes. The dashed lines separate the amphiphatic parts of the helices. (C) Amino acid sequence of the used synthetic peptides. At the critical positions the aa residues of NOS-I are changed into the residues of the NOS-II WT sequence (highlighted in gray). To investigate the importance of single positions, different combinations of aa exchanges are used.

Fluorescence Measurements. Fluorescence experiments were performed similarly as described (*8*, *14*, *25*−*27*) using a Shimadzu RS-1501 fluorescence spectrometer. The excitation wavelength was 335 nm, and the emission spectrum was recorded from 420 to 650 nm. Dansyl-CaM (300 nM) was first measured in buffer with and without calcium in the absence of peptides. Afterward, measurements were done in the presence of varying peptide concentrations. Titration with peptides was performed in 10−30 nM steps until the signal reached saturation. In the case of NOS-I VKFM (Ca^{2+} buffer) smaller steps were used (0.5 nM). Apparent K_D values were determined from dose−reponse curves (two independent titration series). The concentration of free Ca^{2+} in EGTA-containing buffer solution after addition of peptides was checked via determination of the fluorescence lifetime with the Ca^{2+} indicator calcium green 1 (*28*). The free Ca^{2+} in EGTA-buffered solutions was <50 nM and did not change after addition of peptides.

RESULTS

The CaM-binding domains of NOS-I and NOS-II (rat, aa 725−754, and mouse macrophage, aa 503−528, respectively) both harbor hydrophobic amino acids at positions 1, 5, 8, 10, and 14. Therefore, they match both the 1-8-14 and the 1-5-10 recognition motif for Ca^{2+}-dependent binding of CaM (Figure 1A). However, if both domains are displayed in an α-helical wheel plot, some remarkable differences become apparent (Figure 1B). The NOS-I peptide shows a clear segregation of hydrophobic/uncharged and charged amino acids resulting in a typical amphipathic helix. The NOS-II peptide is much more hydrophobic and does not display the

characteristics of an amphipathic helix; only two positively charged amino acids (R and K) are located on one side. Within the 14 amino acid border the main differences in amino acids are K ⇔ V (3), E ⇔ K (6), K ⇔ F (9), and K ⇔ M (13) ,the corresponding positions given in parentheses. We reasoned that these amino acid substitutions might be critical for the different binding of CaM or ApoCaM to NOS isoforms. We synthesized peptides that contained the corresponding point mutations (Figure 1C) and investigated the binding of peptides to CaM and ApoCaM. We also analyzed the thermodynamics of target peptide recognition by CaM and ApoCaM.

Binding of Mutant Peptides to Ca^{2+}-CaM. The interaction of CaM and NOS-I peptides (WT and mutants) was studied by isothermal titration calorimetry (ITC). A typical ITC experiment is seen in Figure 2. CaM was present in the sample cell, and 0.5 or 1 nmol of the peptide in solution was repeatedly injected in constant intervals. Binding of CaM to all four peptides caused exothermic heat pulses (see experiment with NOS-I VKF in Figure 2 A) in the presence of saturating [Ca^{2+}]. The signals decreased to a stable baseline when binding sites were saturated. The molar ratios at which the titration curve reached half-maximal saturation were at 0.8 (NOS-I WT), 0.9 (NOS-I VKF), 1.1 (NOS-I VKFM), and 1.5 (NOS-I E736K) (Figures 2A and 3A).

The average of the baseline was subtracted from the raw data. Integration of the raw data resulted in binding isotherms as shown in Figure 3. Fitting of the S-shaped curves revealed nanomolar affinities for NOS-I WT and the three mutants (Figure 3 and Table 1). In comparison to NOS-I WT the affinity for CaM increased by a factor of 1.2, 3.2, and 14.8 when the CaM-binding sequence was changed at one position (NOS-I E736K), at three positions (NOS-I VKF), and at four positions (NOS-I VKFM), respectively. The binding process was exothermic in the presence of Ca^{2+}. For example, the ΔH for the NOS-I WT was -30.4 kJ mol^{-1} and was very similar to values of ΔH obtained with the mutant peptides of NOS-I (Table 1). All values were between -21.5 kJ mol^{-1} (NOS-I VKFM) and -34.5 kJ mol^{-1} (NOS-I E736K). Values of entropy (ΔS) were rather small but positive between 23.4 and 90.9 J mol^{-1} K^{-1} (Table 1). When in NOS-I WT the negative charge at E736 was changed into a positive (K736), and entropy decreased slightly (Table 1, $\Delta S = 36.2$ J mol^{-1} K^{-1} for NOS-I WT and 23.4 J mol^{-1} K^{-1} for NOS-I E736K). Entropy values increased 2−3-fold when mutant peptides became more hydrophobic by corresponding amino acid substitutions (NOS-I VKF and NOS-I VKFM in Table 1). These experiments indicated that amino acid substitutions at selected positions can significantly increase the apparent binding affinity for CaM and that a change of a charged amino acid to a hydrophobic amino acid has mainly an effect on the ΔS values and almost no effect on ΔH values.

Binding of Mutant Peptides to ApoCaM. Binding of peptides to CaM was further tested in the absence of Ca^{2+}. Titration of ApoCaM by increasing concentrations of mutant peptides yielded ITC signals that saturated at a stable baseline (see, e.g., Figure 2B with peptide NOS-I VKF). The molar ratios at which the titration curves reached half-maximal saturation were 0.9 for NOS-I E736K, 1.3 for NOS-I VKFM, and 1.5 for NOS-I VKF (Figures 2B and 3B). Titration curves were fitted to a one-binding-site reaction (Figure 3B) and yielded apparent K_D values of 1363, 356, and 182 nM

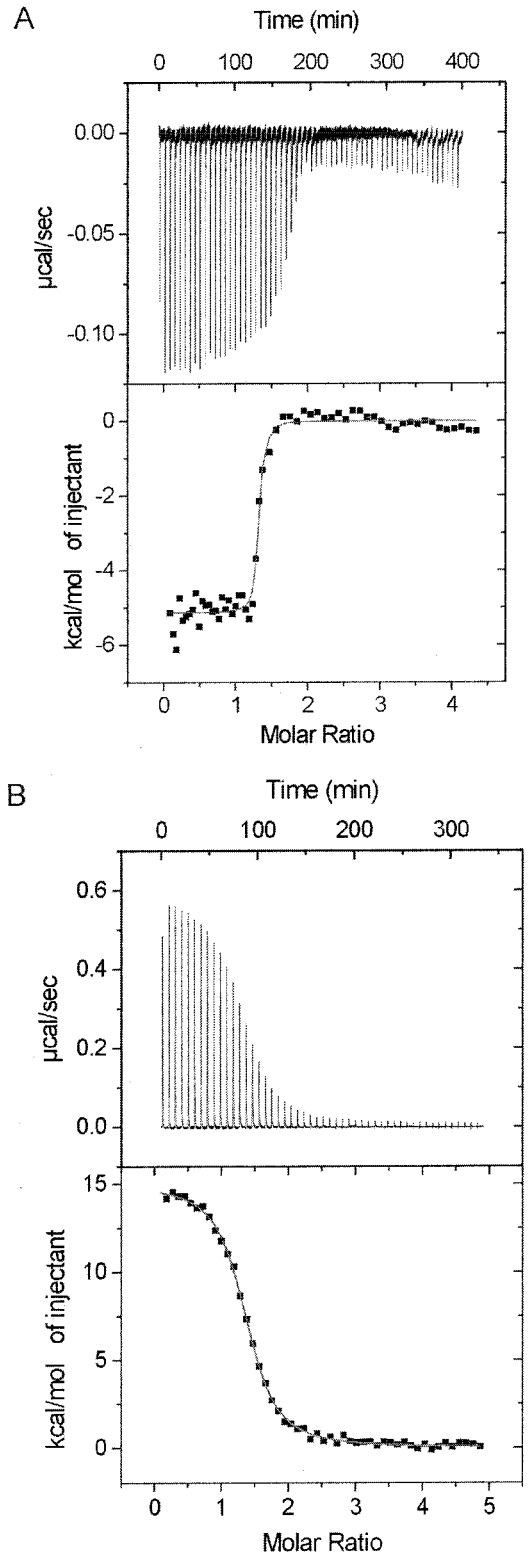

FIGURE 2: Representative ITC measurements with peptide NOS-I VKF and CaM in Ca^{2+} buffer (A) and in EGTA buffer (B). The upper part of each graphic shows the heat pulses (in μcal/s) obtained by repetitive injection of peptide into an 8 μM CaM solution. The lower part of each graphic shows the corresponding changes in enthalpy (kcal/mol of injectants). Data analysis by curve fitting gave the following results for binding of peptide NOS-I VKF to Ca^{2+}-CaM (A), $K_A = 1.16$ e^8 M^{-1}, $K_D = 8.64$ nM, $\Delta H = -21.5$ kJ mol^{-1}, and $\Delta S = 82.3$ J mol^{-1} K^{-1}, and to ApoCaM (B), $K_A = 3.1$ e^6 M^{-1}, $K_D = 326$ nM, $\Delta H = 62.8$ kJ mol^{-1}, and $\Delta S = 334.3$ J mol^{-1} K^{-1}.

Table 1: Thermodynamics of CaM−Peptide Interaction

	peptide	K_A (M^{-1})	K_D (nM)	ΔH (kJ mol^{-1})	ΔS (J mol^{-1} K^{-1})	ΔG (kJ mol^{-1})	*n*
Ca^{2+} buffer	NOS-I WT	$1.6\ e^7 \pm 4.6\ e^6$	64.5 ± 18.8	-30.4 ± 9.2	36.2 ± 30.4[a]	-41.1	7
	NOS-I E736K	$1.8\ e^7 \pm 3.0\ e^6$	54.9 ± 9.2	-34.5 ± 16.3	23.4 ± 53.4[a]	-41.5	2
	NOS-I VKF	$4.9\ e^7 \pm 2.8\ e^7$	20.3 ± 11.7	-29.3 ± 7.9	51.0 ± 31.3	-44.4	2
	NOS-I VKFM	$2.3\ e^8 \pm 1.7\ e^8$	4.4 ± 3.2	-21.5 ± 5.4	90.9 ± 25.7	-48.6	3
EGTA buffer	NOS-I WT						2
	NOS-I E736K[b]	$7.3\ e^5 \pm 3.4\ e^5$	1363 ± 643	29.8 ± 10	213.2 ± 37.2	-33.7	4
	NOS-I VKF	$2.8\ e^6 \pm 2.3\ e^5$	355.5 ± 29.5	57.7 ± 4.9	317.1 ± 17.1	-36.8	2
	NOS-I VKFM[b]	$5.5\ e^6 \pm 1.6\ e^6$	182.1 ± 50.9	55.4 ± 13.6	315.1 ± 45.2	-38.5	3

[a] ΔS changes from positive to negative values in different experiments. [b] Data set obtained from measurements with and without N-terminal Cys.

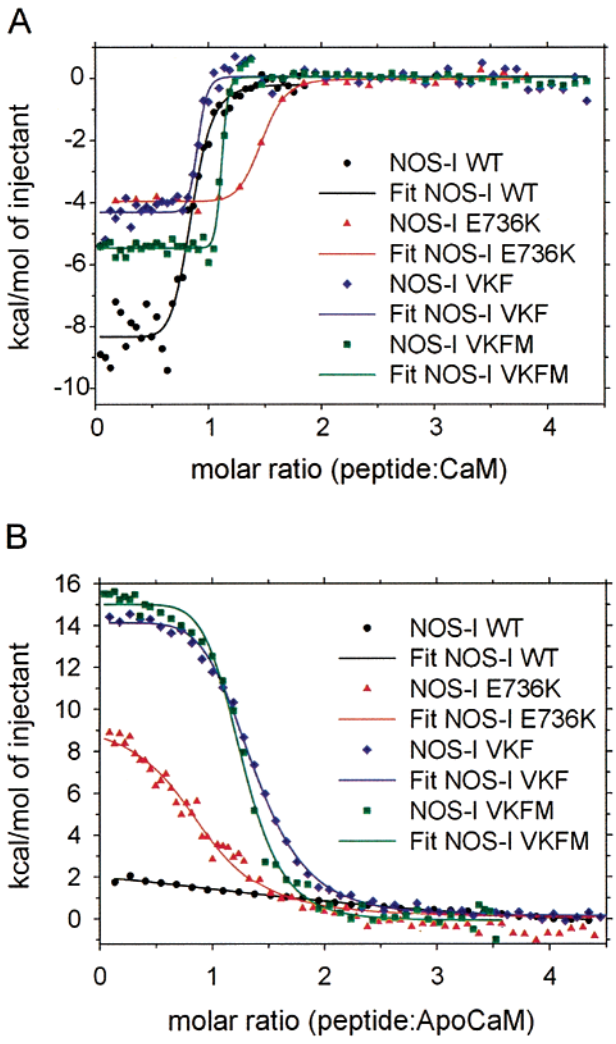

FIGURE 3: Changes in enthalpy (kcal/mol of injectant) are shown as a function of the molar ratios of peptide:CaM (A) and of peptide:ApoCaM (B). Peptides of NOS-I WT and NOS-I mutants were titrated with CaM in the presence and absence of Ca^{2+}. Data were extracted from monitored heat pulses as shown in Figure 2. Symbols indicate experimental data: black circle (●), NOS-I WT; red triangle (▲), NOS-I E736K; blue rectangle (◆), NOS-I VKF; green rectangle (■), NOS-I VKFM.

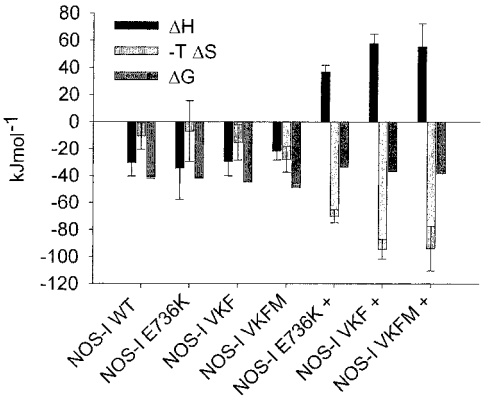

FIGURE 4: Contribution of the enthalpic term (ΔH, black bars) and of the entropic term ($-T\Delta S$, gray) to the Gibbs free energy (ΔG, dark gray). The complex formation of NOS-I peptides and CaM or ApoCaM (addition of EGTA indicated by +) was measured by isothermal titration calorimetry at 25 °C. Values of ΔG were calculated from $\Delta G = \Delta H - T\Delta S$. Values of ΔH and ΔS were taken from Table 1.

for NOS-I E736K, NOS-I VKF, and NOS-I VKFM, respectively (Table 1). We observed endothermic signals of positive ΔH values in case of the mutant peptides (values were between 29.8 kJ mol^{-1} for NOS-I E736K and 57.7 kJ mol^{-1} for NOS-I VKF; Table 1). Changes in entropy were 3−9-fold higher than in experiments with saturating Ca^{2+} (Table 1). Thus, binding of peptides to ApoCaM was mainly entropically driven.

With NOS-I WT no saturation of the binding signal was observed (Figure 3B). The titration of CaM with the peptide resulted in a more or less straight decreasing line that did not display the typical feature of an S-shaped titration curve. These results point to an unspecific aggregation of ApoCaM and NOS-I WT peptide or to a specific interaction with very low affinity.

The contribution of the enthalpic term (ΔH) and the entropic term ($-T\Delta S$) to the Gibbs free energy (ΔG) for each tested peptide of this study is shown in Figure 4. The difference between binding of peptides to CaM and ApoCaM is clearly visible. Values of ΔH are negative for binding to CaM and positive for binding to ApoCaM. The positive values of ΔH are compensated by large positive values of ΔS (large negative contributions of $-T\Delta S$).

Fluorescence Measurements. Dansyl-CaM is widely used to study the interaction of CaM or ApoCaM with target peptides by fluorescence spectroscopy (*8*, *12*, *14*, *25*−*27*). We employed this technique to test the binding of mutant peptides to ApoCaM by a second independent method. Fluorescence emission of dansyl-ApoCaM was maximal at 528 nm. Addition of peptides NOS-I VKFM, NOS-I VKF, and NOS-I E736K shifted the maximum emission wavelength to 506, 497, and 496 nm, respectively (Figure 5). Concomitant with the shift in the maximum wavelength was an increase in intensity, which was 2-fold in the case of

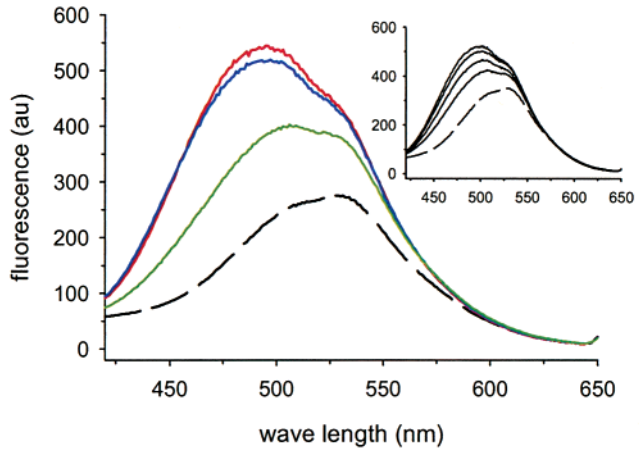

FIGURE 5: Emission fluorescence spectra of dansyl-ApoCaM with and without mutant peptides (E736K, VKF, VKFM). Spectra were recorded with 1 μM ApoCaM (dashed line) and the addition of 2 μM NOS-I E736K (red) or 2 μM NOS-I VKF (blue) or 2 μM NOS-I VKFM (green). Inset: Titration of ApoCaM (1 μM, dashed line) with increasing concentrations of NOS-I WT (1, 2, 3, and 4 μM).

Table 2: Apparent K_D Values Obtained from Titration Experiments with Peptides and Dansyl-CaM

	peptide	K_D (nM)
Ca^{2+} buffer	NOS-I WT	61.5 ± 0.5
	NOS-I E736K	88 ± 9.2
	NOS-I VKF	52 ± 31
	NOS-I VKFM	<1
EGTA buffer	NOS-I WT	
	NOS-I E736K[b]	492 ± 110
	NOS-I VKF	69 ± 52
	NOS-I VKFM[b]	90 ± 7

NOS-I E736K, 1.9-fold in the case of NOS-I VKF, and 1.5-fold in the case of NOS-I VKFM (Figure 5). Thus, binding of mutant peptides to ApoCaM changed the fluorescence emission of dansyl-ApoCaM for each of the three peptides differently. A shift of the maximum wavelength of the fluorescence emission and a change in fluorescence intensity was also observed when Ca^{2+}-CaM bound to NOS-I WT and mutant peptides. We estimated apparent K_D values of peptide binding to Ca^{2+}-CaM and ApoCaM by titration series using 300 nM dansyl-CaM and increasing amounts of peptides. Results are presented in Table 2. Apparent K_D values were of the same order of magnitude as the data obtained by ITC measurements; observed differences were 2.8-fold in the case of NOS-I E736K, 5-fold in the case of VKF, and 2-fold in the case of VKFM (all measurements in EGTA buffer). Thus, the interaction of peptides with Ca^{2+}-CaM and ApoCaM was confirmed by a second independent method. A special case was observed with the NOS-I WT peptide. In the presence of Ca^{2+} fluorescence emission signals saturated at equimolar amounts of NOS-I WT peptide and dansyl-CaM, the apparent K_D value was nearly identical to the value obtained by the ITC experiment (see Table 2). In the absence of Ca^{2+} we repeatedly observed changes in fluorescence emission when peptide was added, but saturation was only approached at roughly 14-fold molar excess of peptide over dansyl-ApoCaM (e.g., titration of NOS-I WT peptide with ApoCaM; see inset in Figure 5).

DISCUSSION

The CaM-binding domain of NOS-I fulfills the criteria of a classical Ca^{2+}-dependent CaM target site. A peptide representing this domain exhibits a reversible interaction of high affinity to CaM, which depends on Ca^{2+}. This interaction is observed in solution (this paper; refs *8*−*10*) and when the NOS-I peptide is immobilized on a SPR biosensor surface and CaM is supplied in the mobile phase (*11*, *29*). A central observation of the presented work is that only a single amino acid substitution of a negative to a positive charge (E736K) can convert this classical Ca^{2+}-dependent CaM-binding site into a target site for ApoCaM. Further substitutions in the CaM-binding site of NOS-I by corresponding amino acids present in the CaM-binding site of NOS-II had mainly an effect on the affinity for ApoCaM and led to a decrease in the apparent K_D.

While a single amino acid substitution determines whether binding of ApoCaM is possible, substitutions at other positions, K ⇔ V (3), K ⇔ F (9), and K ⇔ M (13), increase the apparent affinity of peptides for both Ca^{2+}-CaM and ApoCaM (Table 1). This result shows that the interaction of CaM with target sites can be strengthened by hydrophobic side chains independent of Ca^{2+}. A comparison with CaM-binding sequences in other CaM targets, however, shows that most Ca^{2+}-CaM-binding sites do not harbor a negative charge at the corresponding position of ^{736}E in NOS-I (*1*−*4*). Thus, creation of an apoCaM-binding site by a change from a negative to a positive charge at that position might be special for NOS-I.

Binding of peptides to ApoCaM was in all cases entropically driven, and binding to Ca^{2+}-CaM was enthalpically driven. The entropic term increased with increasing hydrophobicity of peptides (compare E736K with VKF and VKFM) and compensated the positive enthalpic term. Therefore, NOS-I peptide target recognition by Ca^{2+}-CaM is controlled by van der Waals, H-bonding, and electrostatic interactions, whereas binding of peptides to ApoCaM is more dependent on hydrophobic effects, which means that the main contribution of entropy results from the dehydration of exposed hydrophobic amino acid side chains. Although our data on NOS-I related peptides can be grouped into this scheme, previous calorimetric studies of target peptide binding to Ca^{2+}-CaM or ApoCaM have shown that no generalization is warranted, as binding of peptides to Ca^{2+}-CaM and ApoCaM can be both enthalpically and entropically driven processes (*30*−*33*).

Our data do not exclude that the NOS-I WT peptide can bind to ApoCaM with rather low affinity. In fact, heat pulses obtained with NOS-I WT and ApoCaM were clearly different from the baseline, but the resulting binding isotherm was close to a straigth line (Figure 3B). Binding isotherms of this shape indicate very weak or unspecific binding, of which precise values of apparent K_D cannot be obtained (*29*). The observed changes in fluorescence emission with NOS-I WT peptide and dansyl-ApoCaM, which saturated at a ratio of 14:1, do also indicate a weak binding affinity of NOS-I WT peptide for ApoCaM. We can exclude that binding signals originated from a contamination of our solutions with Ca^{2+}, since we verified that EGTA-buffered solutions were essentially Ca^{2+}-free (see Experimental Procedures).

Analysis of the ApoCaM structure has revealed that the N-terminal domain of ApoCaM adopts a closed conformation and the C-terminal domain of ApoCaM a semiopen conformation (*34*−*36*). Binding of a complete IQ motif to ApoCaM occurs via the semiopen conformation of the C-terminal domain and the closed conformation of the N-terminal domain (*37*−*39*). IQ motifs contain an invariant positive charge (R) at position 6 (IQxxx**R**GxxxR). It is striking that the E736K substitution in the NOS-I peptide introduces a positive charge at a corresponding position [if one starts counting from the first hydrophobic anchor ^{732}F in NOS-I (Figure 1A)]. Thus the NOS-I E736K peptide would be similar to the first part of an IQ motif. Since incomplete IQ motifs are predicted to bind to the semiopen conformation of the C-terminal domain of ApoCaM (*37*, *39*), we hypothesize a similar association for the NOS-I E736K to ApoCaM. Hydrophobic patches in the C-terminal domain of ApoCaM are partially surrounded by acidic residues which could be prime candidates for electrostatic interactions with K at position 736. Furthermore, binding of NOS-I E736K to ApoCaM could represent and maybe stabilize a transition state during the Ca^{2+}-triggered conformational change of ApoCaM to Ca^{2+}-CaM.

In addition, peptides could adopt different conformations when they either bind to Ca^{2+}-CaM or ApoCaM. In fact, a study by Yuan et al. (*15*) demonstrated that the NOS-II derived CaM-binding site peptide binds to ApoCaM in a type II β-turn and to Ca^{2+}-CaM in a α-helical conformation. It remains an interesting task to investigate the structure of the NOS-I mutant peptides.

Our data favor a model in which CaM-binding sites can interact with either Ca^{2+}-CaM or ApoCaM, and this interaction solely depends on the amino acids within the binding site. However, this does not exclude any important contributions from other regions in NOS isoforms. In particular, Ca^{2+}-dependent or Ca^{2+}-independent activities could be controlled by other factors or regions as well (*40*−*45*). For example, the endothelial isoform NOS-III is activated in a Ca^{2+}-independent manner upon phosphorylation (*45*).

Finally, we suggest that binding of cellular proteins to ApoCaM is more common as suggested. The ease by which a target site for ApoCaM could be created and the different affinities we have observed with different mutant peptides point to a finely tuned system of ApoCaM-regulated processes. In addition, many proteins could function as "silent" targets, binding to ApoCaM at very low resting free Ca^{2+} concentrations without any activity. When intracellular Ca^{2+} increases, these proteins would become activated without a diffusion-limited delay or they would release Ca^{2+}-CaM for other targets.

ACKNOWLEDGMENT

We thank Prof. M. Bott (IBT, Forschungszentrum Jülich, Germany) for kindly providing us the isothermal titration calorimeter and Dr. T. Gensch (IBI-1, Forschungszentrum Jülich) for advice and help on fluorescence spectroscopy. We also thank D. Höppner-Heitmann for excellent technical assistance.

REFERENCES

1. Rhoads, A. R., and Friedberg, F. (1997) *FASEB J. 11*, 331−340.
2. Jurado, L. A., Chockalingam, P. S., and Jarrett, H. W. (1999) *Physiol. Rev. 79*, 661−682.
3. Crivici, A., and Ikura, M. (1995) *Annu. Rev. Biophys. Biomol. Struct. 24*, 85−116.
4. James, P., Vorherr, T., and Carafoli, E. (1995) *Trends Biochem. Sci. 20*, 38−42.
5. Munshi, H. G., Burks, D. J., Joyal, J. L., White, M. F., and Sacks, D. B. (1996) *Biochemistry 35*, 15883−15889.
6. Cho, H. J., Xie, Q.-W., Calaycay, J., Mumford, R. A., Swiderek, K. M., Lee, T. D., and Nathan, C. (1992) *J. Exp. Med. 176*, 599−604.
7. Griffith, O. W., and Stuehr, D. J. (1995) *Annu. Rev. Physiol. 57*, 707−736.
8. Vorherr, T., Knöpfel, L., Hofmann, F., Mollner, S., Pfeuffer, T., and Carafoli, E. (1993) *Biochemistry 32*, 6081−6088.
9. Zhang, M., and Vogel, H. J. (1994) *J. Biol. Chem. 269*, 981−985.
10. Zhang, M., Yuan, T., Aramini, J. M., and Vogel, H. J. (1995) *J. Biol. Chem. 270*, 20901−20907.
11. Zoche, M., Bienert, M., Beyermann, M., and Koch, K.-W. (1996) *Biochemistry 35*, 8742−8747.
12. Anagli, J., Hofmann, F., Quadroni, M., Vorherr, T., and Carafoli, E. (1995) *Eur. J. Biochem. 233*, 701−708.
13. Stevens-Truss, R., and Marletta, M. A. (1995) *Biochemistry 34*, 15638−15645.
14. Matsubara, M., Hayashi, N., Titani, K., and Taniguchi, H. (1997) *J. Biol. Chem. 272*, 23050−23056.
15. Yuan, T., Vogel, H. J., Sutherland, C., and Walsh, M. P. (1998) *FEBS Lett. 431*, 210−214.
16. Venema, R. C., Sayegh, H. S., Kent, J. D., and Harrison, D. G. (1996) *J. Biol. Chem. 271*, 6435−6440.
17. Stoscheck, C. M. (1990) *Methods Enzymol. 182*, 50−68.
18. Ellmann, G. L. (1959) *Arch. Biochem. Biophys. 82*, 70−77.
19. Wiseman, T., Williston, S., Brandts, J. F., and Lin, L.-N. (1989) *Anal. Biochem. 179*, 131−137.
20. Fisher, H. F., and Singh, N. (1995) *Methods Enzymol. 259*, 194−221.
21. Doyle, M. L. (1997) *Curr. Top. Membr. Transp. 8*, 31−35.
22. Pierce, M. M., Raman, C. S., and Nall, B. T. (1999) *Methods 19*, 213−221.
23. Bradford, M. M. (1976) *Anal. Biochem. 72*, 248−254.
24. Smith, P. K., Krohn, R. I., Hermanson, G. T., Mallia, A. K., Gartner, F. H., Provenzano, M. D., Fujimoto, E. K., Goeke, N. M., Olson, B. J., and Klenk, D. C. (1985) *Anal. Biochem. 150*, 76−85.
25. Kincaid, R. L., Billingsley, M. L., and Vaughan, M. (1988) *Methods Enzymol. 159*, 605−626.
26. Vorherr, T., James, P., Krebs, J., Eyedi, A., McCormick D., Penniston, J. T., and Carafoli, E. (1990) *Biochemistry 29*, 355−365.
27. Liu, M., Chen, T.-Y., Ahamed, B., Li, J., and Yau, K.-W. (1994) *Science 266*, 1348−1354.
28. Schoutteten, L., Denjean, P., Faure, J., and Pansu, R. B. (1999) *Phys. Chem. Chem. Phys. 1*, 2463−2469.
29. Zoche, M., Beyermann, M., and Koch, K.-W. (1997) *Biol. Chem. 378*, 851−857.
30. Wintrode, P. L., and Privalov, P. L. (1997) *J. Mol. Biol. 266*, 1050−1062.
31. Moorthy, A. K., Gopal, B., Satish, P. R., Bhattacharya, S., Bhattacharya, A., Murthy, M. R. N., and Surolia, A. (1999) *FEBS Lett. 461*, 19−24.
32. Tsvetkov, P. O., Protasevich, I. I., Gilli, R., Lafitte, D., Lobachov, V. M., Haiech, J., Briand, C., and Makarov, A. A. (1999) *J. Biol. Chem. 274*, 18161−18164.
33. Brokx, R. D., Lopez, M. M., Vogel, H. J., and Makhatadze, G. I. (2001) *J. Biol. Chem. 276*, 14083−14091.
34. Zhang, M., Tanaka, T., and Ikura, M. (1995) *Nat. Struct. Biol. 2*, 758−767.
35. Kuboniwa, H., Tjandra, N., Grzesiek, S., Ren, H., Klee, C. B., and Bax, A. (1995) *Nat. Struct. Biol. 2*, 768−776.
36. Finn, B. E., Evenäs, J., Drakenberg, T., Waltho, J., Thulin, E., and Forsén, S. (1995) *Nat. Struct. Biol. 2*, 777−783.
37. Houdusse, A., and Cohen, C. (1995) *Proc. Natl. Acad. Sci. U.S.A. 92*, 10644−10647.
38. Houdusse, A., Silver, M., and Cohen, C. (1996) *Structure 4*, 1475−1490.

39. Swindells, M. B., and Ikura, M. (1996) *Nat. Struct. Biol. 3*, 501−504.
40. Ruan, J., Xie, Q.-W., Hutchinson, N., Cho, H., Wolfe, G. C., and Nathan, C. (1996) *J. Biol. Chem. 271*, 22679−22686.
41. Salerno, J. C., Harris, D. E., Irizarry, K., Patel, B., Morales, A. J., Smith, S. M. E., Martasek, P., Roman, L. J., Masters, B. S. S., Jones, C. L., Weissman, B. A., Lane, P., Liu, Q., and Gross, S. S. (1997) *J. Biol. Chem. 272*, 29769−29777.
42. Nishida, C. R., and Ortiz de Montellano, P. R. (1999) *J. Biol. Chem. 274*, 14692−14698.
43. Daff, S., Sagami, I., and Shimizu, T. (1999) *J. Biol. Chem. 274*, 30589−30595.
44. Montgomery, H. J., Romanov, V., and Guillemette, J. G. (2000) *J. Biol. Chem. 275*, 5052−5058.
45. Butt, E., Bernhardt, M., Smolenski, A., Kotsonis, P., Fröhlich, L. G., Sickmann, A., Meyer, H. E., Lohmann, S. M., and Schmidt, H. H. H. W. (2000) *J. Biol. Chem. 275*, 5179−5187.

BI025681K